Signal Statistics in Fiber-Optical Channels With Polarization Multiplexing and Self-Phase Modulation

Lotfollah Beygi, Erik Agrell, Magnus Karlsson, and Pontus Johannisson

***Abstract*—In this paper, the statistics of received signals in a single-channel dispersion-managed dual-polarization fiber-optical channel are derived in the limit of low dispersion. The joint probability density function (pdf) of the received amplitudes and phases of such a system is derived for both lumped and distributed amplification. The new pdf expressions are used to numerically evaluate the performance of modulation formats over channels with nonlinear phase noise. For example, a sensitivity gain of up to 2 dB is calculated for a specific system using polarization-multiplexed 8-ary phase-shift keying compared with a similar single-polarization system at the same spectral efficiency and a symbol error rate of 5×10^{-4}. Moreover, the accuracy of the derived pdf is evaluated for some single-channel dispersion-managed fiber-optical links with different dispersion maps using the split-step Fourier transform method.**

***Index Terms*—Dual polarization, nonlinear optics, optical fiber communication, optical Kerr effect, phase noise, polarization multiplexing, probability density function (pdf), self-phase modulation, signal statistics.**

I. Introduction

THE HIGH demand for increasing the data rate of fiber-optical channels imposes utilizing all resources in these channels. Recently, extensive efforts see, e.g., [1]–[4] have been devoted to utilizing both polarizations of an optical signal in a fiber channel to convey information. The dual polarization (DP) scheme makes it possible to exploit all degrees of freedom in a fiber-optical channel to boost the data rate [5], [6]. A DP signal can be modeled in a 4-D signal space [7], [8], which yields a more power-efficient scheme for a fixed spectral efficiency by exploiting dense sphere packing constellations.

In a long-haul dispersion-managed (DM) fiber-optical channel, the nonlinear phase noise (NLPN) (see [9] ch. 4) is a major impairment for phase-modulated signals. NLPN is generated by the interaction of a signal and amplified spontaneous emission (ASE) noise from the optical amplifiers, due to the nonlinear Kerr effect. Gordon and Mollenauer [10] first showed this phenomenon in a fiber link with many spans, in which optical amplifiers are used to periodically compensate for fiber loss. This effect is known as self-phase modulation and causes a major degradation in the performance of coherent single-channel data transmission systems.

Bononi *et al.* [11] studied the resilience of ON–OFF keying, incoherent differential binary and quadrature phase-shift keying (D(Q)PSK), and DSP-based coherent polarization multiplexed QPSK (PDM-QPSK) to NLPN in a DM fiber link. They provided a quantitative understanding of the system parameters for which NLPN sets the nonlinear performance of these modulation formats.

The characteristic function (i.e., the Fourier transform of pdf) of NLPN for a single-polarization (SP) system has been studied analytically in [12]–[15] by taking into account the correlation of the NLPN and the intensity of the received signal. Moreover, the statistics of NLPN have been evaluated experimentally in [16]. It was shown in [13], [14], and [17] that the NLPN distribution cannot be approximated by a Gaussian distribution.

In [18], a technique based on Gauss–Hermite basis functions was used to calculate the variance of phase noise in a coherent system based on phase-shift keying (PSK). A comprehensive methodology and computational techniques for the analysis and characterization of NLPN phenomena and their impact on system performance have been presented in [19], based on a linear perturbation/noise theory.

In order to evaluate the performance of a phase-modulated signal, knowledge of the probability density function (pdf) of the received phase, consisting of both NLPN and linear phase, is necessary. Due to the dependence between NLPN and the phase of amplifier noise, the joint pdf of these two terms should be computed. Mecozzi derived this joint pdf for distributed amplification in [12], [17] and Ho (see [20] ch. 5) developed this joint pdf for both distributed and lumped amplifications. The exact performance of PSK systems is computed exploiting this joint pdf in ([20] ch. 6).

The joint pdf of the received amplitude and phase given the initial phase of the transmitted signal and the signal-to-noise ratio (SNR) was derived in ([20] ch. 5) for a fiber channel with NLPN caused by distributed or lumped amplification. This joint pdf was used to evaluate the performance of a quadrature amplitude modulated (QAM) signal in a fiber-optical channel with NLPN. Although the statistics of the received signal provide a possibility of designing a maximum-likelihood (ML) receiver for QAM signals, the analytical computation of the exact performance of these systems is still cumbersome. Moreover, the compensation of the NLPN has been studied in [21] and [22] based on the aforementioned pdf.

In this paper, we extend the statistics of the SP system to the DP scheme for a fiber-optic channel with low dispersion. The

Manuscript received January 27, 2011; revised April 19, 2011, June 02, 2011; accepted June 06, 2011. Date of publication June 16, 2011; date of current version July 27, 2011. This work was supported by the Swedish Research Council under Grant 2007-6223.

The authors are with the Chalmers University of Technology, Gothenburg 41276, Sweden (e-mail: beygil@chalmers.se; agrell@chalmers.se; magnus.karlsson@chalmers.se; pontus.johannisson@chalmers.se).

Color versions of one or more of the figures in this paper are available online at http://ieeexplore.ieee.org.

Digital Object Identifier 10.1109/JLT.2011.2159777

joint pdf of the received amplitudes and phases of the orthogonal polarizations, denoted by *x* and *y*, is derived analytically. These statistics are introduced for both types of amplification, i.e., lumped and distributed. The derived statistics provide the possibility of comparing the performance of SP and DP systems for different system configurations. Some numerical results are given for the symbol error rate (SER) of the DP system with an 8-ary phase-shift keying (8-PSK) signal set in each polarization. According to these numerical results, the DP scheme is superior to SP for a fixed spectral efficiency.

To verify the accuracy of the exploited fiber-optic model with low dispersion (see Section II), a general model of a DM fiber-optic link, consisting of a number of spans with optical amplifiers, single-mode fiber (SMF), and dispersion-compensation fibers (DCF) is considered. For a DM link, the pdf of the received signal will converge to a Gaussian-like pdf at high-enough symbol rates [11], [15]. Therefore, the derived pdf is a good approximation at low symbol rates for a DM fiber-optical link. The numerical results reveal that the exploited fiber-optic model with low dispersion (see [20], p. 154), [10], [17], [21], [22] is not sufficiently accurate for increased symbol rates in a DM fiber-optical link due to the high group velocity dispersion.

This paper is organized as follows. In Section II, we describe the system model for a DP fiber-optic channel with low dispersion. The derivation of statistics of this channel for NLPN alone is described in Section III. The joint pdf of the received amplitudes and phases of the received signal for a DP signal is performed in Section IV. We exemplify the use of the derived pdf in the SER evaluation of a particular systems with 8-PSK modulation in Section V for a fiber-optic link with low dispersion and then by using a general model based on the split-step Fourier method (SSFM) (see[9], ch. 2), the accuracy of the simplified model is studied for some DM links. Finally, Section VI concludes this paper.

II. System Model

We neglect the effect of chromatic dispersion in this paper, which makes this analysis applicable to fiber-optic systems with low dispersion, similarly as, e.g., [10], [17], [21], [22]. However, we will evaluate the effect of chromatic dispersion on the validity of this model for a DM fiber-optical link by exploiting some numerical simulations with the SSFM.

A. Fiber-Optic Channel With Low Dispersion

For a zero polarization mode and chromatic dispersion fiber-optical channel, the nonlinear Schrödinger equation which describes the light propagation in an optical fiber is (see [9], ch. 6)

$$j\frac{\partial \mathbf{E}}{\partial z} + \gamma(\mathbf{E}\mathbf{E}^{\dagger})\mathbf{E} + j\frac{\alpha}{2}\mathbf{E} = \mathbf{0} \tag{1}$$

where $\mathbf{E} = (E_x, E_y)$ is the dual polarized launched envelope signal into the fiber channel, γ is the fiber nonlinear coefficient, α is the attenuation coefficient of the fiber, $\dagger$ denotes the Hermitian conjugation, and z is the distance from the beginning of the fiber. The solution to (1) at time t can be written as

$$\mathbf{E}(z,t) = \mathbf{E}(0,t)q(z)\exp\left(j\gamma P_0(t)\int_0^z q^2(\tau)d\tau\right) \tag{2}$$

where $P_0(t) = |E_x(0,t)|^2 + |E_y(0,t)|^2$ is the instantaneous launched power into the fiber and $q(z) = \exp(-\alpha z/2)$ is a function that describes the power evolution.

Here, we assume a fiber link with total length L, N spans with lumped amplifiers, where the fiber loss is compensated perfectly. Each amplifier adds complex circularly symmetric Gaussian ASE noise n_x^k and n_y^k, $k = 1, \ldots, N$ in the polarization *x* and *y*, respectively, with variance σ_0^2. Moreover, we consider the noise within the optical signal bandwidth, i.e., ignoring the Kerr effect induced from out-of-band signal and noise in a same way as [10].

If a 4-D signal $\mathbf{S} = (S_x, S_y)$, consisting of 2-D components from a signal set $\mathcal{M}$, is transmitted on the two orthogonal polarizations, *x* and *y*, of a fiber channel, it is readily seen that each fiber span according to (2) contributes the overall NLPN [10] $\varphi = \gamma P_k L_{\text{eff}}$ to the transmitted signal, where

$$L_{\text{eff}} = \int_0^{L/N} q^2(z)dz = \frac{1}{\alpha}\left[1 - \exp\left(-\frac{\alpha L}{N}\right)\right]$$

is the effective nonlinear length of each span and $P_k = |S_x + \sum_{i=1}^k n_x^i|^2 + |S_y + \sum_{i=1}^k n_y^i|^2$ is the input power of the kth fiber span. The transmitted 4-D signal experiences the total NLPN of $\phi_n = \phi_x + \phi_y$[1]. The terms ϕ_x and ϕ_y are generated by interaction of the signal and noise due to Kerr effect in the polarizations *x* and *y*, respectively. This reveals the fact that signals in both polarizations contribute to the generated NLPN ϕ_n. Due to symmetry, we show the derivations for the polarization *x* only, while one may easily find the results for the other polarization by replacing *x* with *y*.

$$\phi_x = \gamma L_{\text{eff}} \sum_{i=1}^{N} \left| S_x + \sum_{k=1}^{i} n_x^k \right|^2 \tag{3}$$

The received electric field $\mathbf{E}$ can be written as[2]

$$\mathbf{E} = \hat{\mathbf{E}} e^{-j\phi_n} \tag{4}$$

where $\hat{\mathbf{E}} = \mathbf{S} + \sum_{k=1}^N \mathbf{n}^k$ is the linear part of the electric field and $\mathbf{n}^k = (n_x^k, n_y^k)$. One may consider the distributed amplification as a discrete lumped amplification with an infinite number of spans. This gives $\lim_{N\to\infty} N L_{\text{eff}} = L$. In this case, a continuous amplifier noise vector $\mathbf{n}(z) = (n_x(z), n_y(z))$ is considered with elements as zero-mean complex-valued Wiener processes with autocorrelation function ([20], p. 154)

$$\mathrm{E}[n_x(z_1)n_x^*(z_2)] = \sigma_d^2 \min(z_1, z_2)$$

[1]Here, we have used (6.2.5) of [9] with $B = 1$ based on the Manakov model [23].

[2]By definition, $E = E(L,t)$ is a time-dependent electric field, not a vector representation of the projected received electric field in a signal space. We nevertheless use (4) to model the discrete-time system, where E is a complex signal vector. This is a standard approximation in the field and has been shown numerically [24], [25] to be reasonably accurate, although the theoretical justification is insufficient

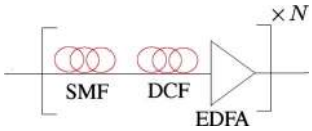

Fig. 1. DM fiber-optical link with N spans. Each span consists of an SMF, a DCF, and an EDFA.

TABLE I
SIMULATED DM SYSTEMS

System	I	II	III	IV	V	VI	VII
Symbol rate (Gbaud)	6	10	15	20	3	5	7
D (ps/nm/km)	3	3	3	3	16.5	16.5	16.5
n_{sp}	3.2	3.2	3.2	3.2	1.4	1.4	1.4
N_{Span}	25	14	10	8	25	22	14

where $\sigma_d^2 = N\sigma_0^2/L$. The NLPN can be computed for distributed amplification by

$$\phi_n = \frac{\gamma N L_{\text{eff}}}{L}\int_0^L \|\mathbf{S}+\mathbf{n}(z)\|^2 dz. \tag{5}$$

The ASE noise $n_x(L)$ and $n_y(L)$ generated by in-line amplifiers in polarization x and y, respectively, and accumulated at the receiver have the variance $L\sigma_d^2 = 2h\nu_{\text{opt}}WL\alpha n_{\text{sp}}$ [21], where $h\nu_{\text{opt}}$ is the energy of a photon, n_{sp} is the spontaneous emission factor, and W is the bandwidth of the optical signal. The SNR vector is defined as $\rho = (\rho_x, \rho_y)$ where ρ_x is $|S_x|^2/(L\sigma_d^2)$ or $|S_x|^2/(N\sigma_0^2)$ for distributed or lumped amplification, respectively.

B. DM Fiber-Optical Channel

We consider a general DM fiber link with N spans in which an SMF and a DCF is used according to a dispersion map (see Table I). The dispersion of each span is fully compensated by a DCF fiber and neither precompensation nor postcompensation is used. An erbium doped fiber amplifier (EDFA) compensates for the fiber loss in each span. The SSFM is used to simulate a DM fiber-optical link shown in Fig. 1. The following channel parameters are used for the numerical simulations: the nonlinear coefficients $\gamma_{\text{SMF}} = 1.4$ and $\gamma_{dCF} = 5.2\text{W}^{-1}\cdot\text{km}^{-1}$, the optical frequency $\nu_{\text{opt}} = 193.55$ THz, the attenuation coefficients $\alpha_{\text{SMF}} = 0.25$ and $\alpha_{dCF} = 0.6$ dB/km, the dispersion coefficient $D_{dCF} = -120$ ps/nm/km, and the fiber lengths $L_{\text{SMF}} = 80$ km. The rest of the parameters are given in Table I for the numerical simulations (see Section V).

III. NLPN

In this section, we extend the results of ([20] ch. 5) to DP signals. Due to the difficulty of computing the pdf of ϕ_n directly, we first compute the characteristic function. Since $n_x(z)$ and $n_y(z)$ are independent, ϕ_x and ϕ_y are also independent. Therefore, the pdf of ϕ_n can be obtained by the convolution of the pdfs of ϕ_x and ϕ_y, or the product of their characteristic functions [26]

$$\Psi_{\Phi_n}(\nu) = \Psi_{\Phi_x}(\nu)\Psi_{\Phi_y}(\nu). \tag{6}$$

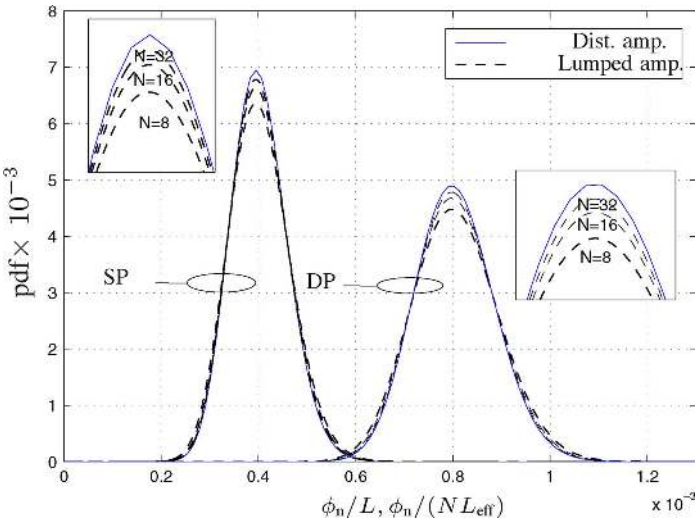

Fig. 2. Pdfs of the normalized NLPN for a fiber-optic link with low dispersion and distributed (ϕ_n/L) and lumped ($\phi_n/(NL_{\text{eff}})$; $N = 8, 16$, and 32) amplification ($\rho_x = \rho_y = 15$ dB, $L = 4000$ km, and $R_s = 10$ Gbaud).

A. Distributed Amplification

For distributed amplification, the characteristic function of ϕ_x is given in ([20], p. 157)[3]

$$\Psi_{\Phi_x}(\nu) = \sec(L\sigma_d\sqrt{j\gamma\nu}) \times \exp\left(\rho_x L\sigma_d\sqrt{j\gamma\nu}\tan(L\sigma_d\sqrt{j\gamma\nu})\right). \tag{7}$$

One may interchange x and y in (7) to obtain Ψ_{Φ_y} and by substituting Ψ_{Φ_x} and Ψ_{Φ_y} into (6), we get

$$\Psi_{\Phi_n}(\nu) = \sec^2(L\sigma_d\sqrt{j\gamma\nu}) \times \exp\left((\rho_x+\rho_y)L\sigma_d\sqrt{j\gamma\nu}\ \tan(L\sigma_d\sqrt{j\gamma\nu})\right). \tag{8}$$

The pdf of the NLPN is illustrated in Fig. 2 for $\text{SNR} = 15$ dB by taking the inverse Fourier transform of (8). The mean and the variance of the NLPN can be obtained as

$$\mathbb{E}\{\Phi_n\} = -j\frac{d}{d\nu}\Psi_{\Phi_n}(\nu)\Big|_{\nu=0} = \gamma L^2\sigma_d^2(\rho_x+\rho_y+1) \tag{9}$$

and

$$\sigma^2_{\Phi_n} = \gamma^2 L^4\sigma_d^4\left(\frac{2}{3}(\rho_x+\rho_y)+\frac{1}{3}\right) \tag{10}$$

where we used $\mathbb{E}\{\Phi_n^2\} = -j(d^2)/(d\nu^2)\Psi_{\Phi_n}(\nu)|_{\nu=0}$. As seen in Fig. 2, the mean and the variance of the NLPN have been doubled for the DP case compared with SP ([20] p. 157) provided that the transmitted signals in both polarizations have the same SNR.

B. Lumped Amplification

The characteristic function of NLPN for an SP system with lumped amplification is given in ([20] ch. 5) by

$$\Psi_{\Phi_n}(\nu) = \prod_{k=1}^{N}\frac{1}{1-j\gamma L_{\text{eff}}\nu\lambda_k\sigma_0^2} \times \exp\left(\frac{j\gamma\nu|S_x|^2L_{\text{eff}}(\mathbf{\Lambda}_k\cdot\chi)^2}{\lambda_k - j\gamma L_{\text{eff}}\nu\lambda_k^2\sigma_0^2}\right) \tag{11}$$

[3]In contrast to [20], we have removed the normalization factor γL_{eff} in (7) and (11).

where $\chi = (N, N-1, \ldots, 2, 1)^T$, $\cdot$ is the inner product of two real vectors, and λ_k and $\mathbf{\Lambda}_k$ are the eigenvalues and eigenvectors, respectively, of the covariance matrix ([20] p. 149)

$$\mathbf{\Pi} = \begin{pmatrix} N & N-1 & N-2 & \ldots & 1 \\ N-1 & N-1 & N-2 & \ldots & 1 \\ \vdots & \vdots & \vdots & \ddots & \vdots \\ 1 & 1 & 1 & \ldots & 1 \end{pmatrix}.$$

The characteristic function of the NLPN for a DP system with lumped amplification can be derived by an analogous approach as Section III-A and using (11) as

$$\Psi_{\Phi_n}(\nu) = \prod_{k=1}^{N} \frac{1}{\left(1 - j\gamma L_{\text{eff}} \nu \lambda_k \sigma_0^2\right)^2} \times \exp\left(\frac{j\gamma\nu \|\mathbf{S}\|^2 L_{\text{eff}} (\mathbf{\Lambda}_k \cdot \chi)^2}{\lambda_k - j\gamma L_{\text{eff}} \nu \lambda_k^2 \sigma_0^2}\right). \quad (12)$$

The mean and the variance of the NLPN for a DP system with lumped amplification can be readily obtained exploiting the results for an SP system in ([20] sec. 6.2), as

$$\mathbb{E}\{\Phi_n\} = N\gamma L_{\text{eff}} \left(\|\mathbf{S}\|^2 + 2(n+1)\sigma_0^2\right) \quad (13)$$

and

$$\sigma_{\Phi_n}^2 = \frac{4}{3} N(N+1)(\gamma L_{\text{eff}} \sigma_0)^2 \times \left[\left(N + \frac{1}{2}\right)\|\mathbf{S}\|^2 + 2(N^2+N+1)\sigma_0^2\right]. \quad (14)$$

Analogously, it can be shown using (13) and (14) that the mean and the variance of NLPN of a DP system are twice of those for an SP system, which was first shown in [27]. As seen in Fig. 2, the pdf of NLPN for a lumped amplification will be overlapped with distributed one for $N > 32$. The pdf of the NLPN is plotted by taking the inverse Fourier transform of the characteristic functions (8) and (12). As seen in Fig. 2, the DP scheme has larger mean and variance than the SP system.

IV. Joint PDF of the Received Amplitudes and Phases of the DP Signal

In the SP case, the system transmits in only one polarization and the joint pdf of the amplitude and the phase of the received signal is ([20] p. 225)

$$f_{\Theta_x, R_x}(\theta_x, r_x) = \frac{f_{R_x}(r_x)}{2\pi} + \frac{1}{\pi}\sum_{k=1}^{\infty} \text{Re}\left\{C_k^x(r_x) e^{jk\theta_x}\right\} \quad (15)$$

where the normalized received amplitude r_x is denoted by $|E_x|/(\sigma_d\sqrt{L})$ and $|E_x|/(\sigma_0\sqrt{N})$ for distributed and lumped amplifications, respectively. Here, the induced phase noise from the noise of the orthogonal polarization and the out-of-band noise is ignored. Moreover, $f_R(r) = 2re^{-(r^2+\rho^2)} I_0(2r\sqrt{\rho})$ is the Ricean pdf and the coefficients C_k^x of the polarization x for both types of amplifications is obtained as

$$C_k^x(r_x) = \frac{r_x \Psi_\Phi(k)}{\tau^2(k)} \times \exp\left(-\frac{r_x^2 + m_x^2(k)}{2\tau^2(k)}\right) I_k\left(\frac{m_x(k) r_x}{\tau^2(k)}\right), \quad (16)$$

where $I_q(\cdot)$ denotes the qth-order modified Bessel function of the first kind. For distributed amplification

$$\tau^2(\nu) = \tan(L\sigma_d\sqrt{j\gamma\nu})/(2L\sigma_d\sqrt{j\gamma\nu}) \quad (17)$$

$$m_x(\nu) = \sqrt{\rho_x}\sec\left(L\sigma_d\sqrt{j\gamma\nu}\right) \quad (18)$$

and $\Psi_{\Phi_n}(j\nu)$ is given in (7). In the case of lumped amplification

$$\tau^2(\nu) = \sigma_0^2 \sum_{k=1}^{N} \frac{(\mathbf{\Lambda}_k \cdot \chi)^2}{1 - j\nu\gamma L_{\text{eff}} \lambda_k \sigma_0^2} \quad (19)$$

$$m_x(\nu) = S_x \sum_{k=1}^{N} \frac{(\mathbf{\Lambda}_k \cdot \chi)(\mathbf{\Lambda}_k \cdot \mathbf{\Gamma})/\lambda_k}{1 - j\nu\gamma L_{\text{eff}} \lambda_k \sigma_0^2} \quad (20)$$

in which $\mathbf{\Gamma} = (1, 1, \ldots, 1)^T$, and $\Psi_{\Phi_n}(j\nu)$ is given in (11). Here, the statistics of a DP 4-D signal after propagation through a DM fiber channel are derived for distributed and lumped amplification. The motivation for deriving $f_{\mathbf{\Theta},\mathbf{R}}(\theta, \mathbf{r})$, i.e., the joint pdf of the normalized received amplitudes $\mathbf{r} = (r_x, r_y)$ and phases $\theta = (\theta_x, \theta_y)$, is to design an ML receiver for such systems. The joint pdf of the two normalized independent Ricean random variables r_x and r_y can be written by ([28] p. 50)

$$f_{\mathbf{R}}(\mathbf{r}) = 4r_x r_y e^{-(\|\mathbf{r}\|^2 + \rho_x + \rho_y)} I_0(2r_x\rho_x) I_0(2r_y\rho_y). \quad (21)$$

According to the model (4), the received phase vector θ is the sum of the transmitted phase vector, the phase vector of the received linear part $\hat{\theta} = (\hat{\theta}_x, \hat{\theta}_y)$, and the NLPN vector (ϕ_n, ϕ_n). Without loss of generality, we assume the transmitted phase vector to be (0,0). Therefore, we have

$$\theta = \hat{\theta} - (\phi_n, \phi_n). \quad (22)$$

Theorem 1: The joint pdf of the received phase vector θ and the normalized amplitudes $\mathbf{r}$ of a DM fiber channel with *distributed amplification* is

$$\begin{aligned} f_{\mathbf{\Theta},\mathbf{R}}(\theta, \mathbf{r}) &= \frac{f_{\mathbf{R}}(\mathbf{r})}{4\pi^2} + \frac{1}{2\pi^2}\sum_{k_x=1}^{\infty} \text{Re}\{C_{\mathbf{k}_x}(\mathbf{r}) e^{jk_x\theta_x}\} \\ &\quad + \frac{1}{2\pi^2}\sum_{k_x=1}^{\infty}\sum_{k_y=1}^{\infty} \text{Re}\left\{C_{\mathbf{k}}(\mathbf{r}) e^{j\mathbf{k}\cdot\theta} + C_{\mathbf{k}^*}(\mathbf{r}) e^{j\mathbf{k}^*\cdot\theta}\right\} \\ &\quad + \frac{1}{2\pi^2}\sum_{k_y=1}^{\infty} \text{Re}\{C_{\mathbf{k}_y}(\mathbf{r}) e^{jk_y\theta_y}\} \end{aligned} \quad (23)$$

where

$$C_{\mathbf{k}}(\mathbf{r}) = \frac{r_x r_y \Psi_{\Phi_n}(k_{xy})}{\tau^4(k_{xy})} \exp\left(-\frac{\|\mathbf{r}\|^2 + \|\mathbf{m}(k_{xy})\|^2}{2\tau^2(k_{xy})}\right) \times I_{k_x}\left(\frac{m_x(k_{xy}) r_x}{\tau^2(k_{xy})}\right) I_{k_y}\left(\frac{m_y(k_{xy}) r_y}{\tau^2(k_{xy})}\right). \quad (24)$$

Here, $\mathbf{k} = (k_x, k_y)$ is a vector with positive integer elements, $\mathbf{k}_x = (k_x, 0)$, $\mathbf{k}_y = (0, k_y)$, $\mathbf{k}^* = (k_x, -k_y)$, $k_{xy} = k_x + k_y$, $\mathbf{m}(\nu) = (m_x(\nu), m_y(\nu))$, $\tau(\nu)$, and $m_x(\nu)$ are given in (17)–(18), and $\Psi_{\Phi_n}(j\nu)$ is given in (8).

Proof: See Appendix A. ■

Theorem 2: In the case of *lumped amplification*, the joint pdf of the received phase vector θ and normalized amplitudes $\mathbf{r}$ of a

DM fiber channel is given by (23)–(24), where $\tau(\nu)$ and $m_x(\nu)$ are given in (19) and (20), $\Psi_{\Phi_n}(j\nu)$ is given in (12), and the rest of the parameters are the same as in Theorem 1.

Proof: The proof is analogous to Theorem 1, exploiting the results of ([20] p. 185) for a finite number of spans with lumped amplification. ■

Interestingly, the Fourier series coefficients $C_{\mathbf{k}}$ for a DP system are the product of the Fourier series coefficients of the two polarizations *x* and *y* as

$$C_{\mathbf{k}}(\mathbf{r}) = C^x_{\mathbf{k}}(r_x)C^y_{\mathbf{k}}(r_y). \tag{25}$$

The coefficients $C^x_{\mathbf{k}}(r_x)$ of the polarization *x* for both types of amplifications are

$$C^x_{\mathbf{k}}(r_x) = \frac{r_x \Psi_\Phi(k_{xy})}{\tau^2(k_{xy})} \exp\left(-\frac{r_x^2 + m_x^2(k_{xy})}{2\tau^2(k_{xy})}\right) \times I_{k_x}\left(\frac{m_x(k_{xy})r_x}{\tau^2(k_{xy})}\right). \tag{26}$$

Hence, the coefficients $C^x_{k_x}$ of (16) for an SP system can be obtained as a special case of (26) by setting $\mathbf{k} = \mathbf{k}_x$.

The marginal joint pdf of the amplitude and the phase of the received signal for solely polarization *x* can be obtained from (23), (24), and (25) as

$$f_{\Theta_x,R_x}(\theta_x, r_x) = \frac{f_{R_x}(r_x)}{2\pi} + \frac{1}{\pi}\sum_{k_x=1}^{\infty} \mathrm{Re}\left\{C'_{\mathbf{k}_x}(r_x)e^{jk_x\theta_x}\right\} \tag{27}$$

where

$$C'_{\mathbf{k}_x}(r_x) = C^x_{\mathbf{k}_x}(r_x)\int_{r_y=0}^{\infty} C^y_{\mathbf{k}_x}(r_y)dr_y.$$

V. Numerical Results

In this section, we first compare the SER performance of an SP and a DP fiber-optic link with low dispersion to evaluate the SER degradation due to the NLPN contribution from the two polarizations. Then, we check the accuracy of the exploited model for DM fiber-optical links of Table I.

A. Fiber-Optic Channel With Low Dispersion

The performance of a polarization-multiplexed 8-PSK (PM-8PSK) [29] modulation format is evaluated by simulations. The approach proposed in [21] is implemented to attain a very low complex ML detector based on the pdf derived in Theorem 1. We compute the SER of PM-8PSK and compare it with SP 8-PSK for the same power P_t per polarization. The exploited symbol-by-symbol[4] ML detector uses the derived pdf to detect the received 4-D symbol $\tilde{\mathbf{S}}$ by

$$\tilde{\mathbf{S}} = \arg\max_{\mathbf{S}\in\mathcal{M}} f_{\mathbf{\Theta}-\mathbf{\Theta}^0,\mathbf{R}}(\theta, \mathbf{r}) \tag{28}$$

where $f_{\mathbf{\Theta}-\mathbf{\Theta}^0,\mathbf{R}}$ is the joint pdf of the differential received phases and amplitudes of both polarizations in Theorem 1. Here, $\mathbf{\Theta}^0$ is the initial phase vector (i.e., at the transmitter) of the transmitted symbols of both polarizations which was assumed to be $\mathbf{0}$ in Theorem 1. The signal set $\mathcal{M}$ denotes the 4-D constellation, i.e., $(8\text{-PSK})^2$ in our numerical analysis. This evaluation is done for distributed amplification with no dispersion similarly to [21], [22] (system VI). In Fig. 3, the SER performance is plotted versus transmitted power per polarization for the SP and DP systems with zero dispersion, 10 Gbaud, $N_{\mathrm{span}} = 50$, and 8-PSK constellation. As seen in this figure, the DP scheme shows a negligible performance degradation ($\cong 0.25$ dB) in the linear regime at the same symbol rate R_s and $\mathrm{SER} = 5 \times 10^{-4}$, while for a fixed spectral efficiency, one may observe a $5 - 3 = 2$ dB performance improvement in exploiting the DP scheme rather than SP (to compare at the same transmitted power, the DP curve in Fig. 3 should be shifted 3 dB to the right). This result has been demonstrated previously in [30]. Moreover, the SP 8-PSK system with symbol rate $2R_s$ does not go below $\mathrm{SER} = 5 \times 10^{-4}$ for any power, while DP 8-PSK reaches a minimum of 3×10^{-5}. As expected in the nonlinear regime, the SP scheme is superior to the DP case at the expense of losing half of the spectral efficiency.

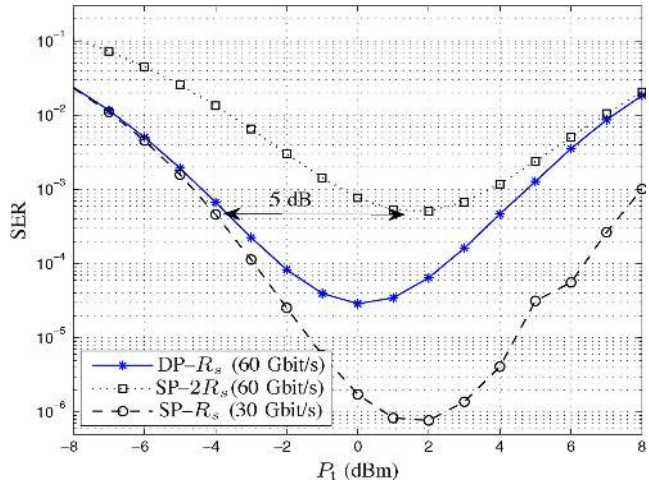

Fig. 3. SER of a fiber-optic link with zero dispersion, 10 Gbaud, and $N_{\mathrm{span}} = 50$ for DP and SP 8-PSK constellation versus transmitted power per polarization P_t.

Another interesting point is the convergence of DP-R_s and SP-R_s at low P_t and the convergence of DP-R_s and SP-$2R_s$ at high P_t, as seen in Fig. 3. The convergence at low P_t is due to disappearing nonlinear effects in this regime. At high P_t, the major impairment is NLPN, which is a function of the transmitted signal power and the added noise power in both polarizations. In the DP system, the total transmitted power is twice the power in the SP system. On the other hand, doubling the symbol rate will boost the noise power by a factor of 2 for the SP system. Therefore, the high-power SER performance will be the same for the DP-R_s and SP-$2R_s$ systems.

B. DM Channel

To verify the accuracy of the theoretical pdf derived in Theorem 1 for different scenarios, we compare it with the numerical pdf estimated from extensive numerical simulations. The SSFM ([9] ch. 2) is exploited to implement the fiber-optical channel for the systems given in Table I. In this table, we have considered

[4]We use an uncoded scheme and the detector is memoryless (not an ML sequence detector).

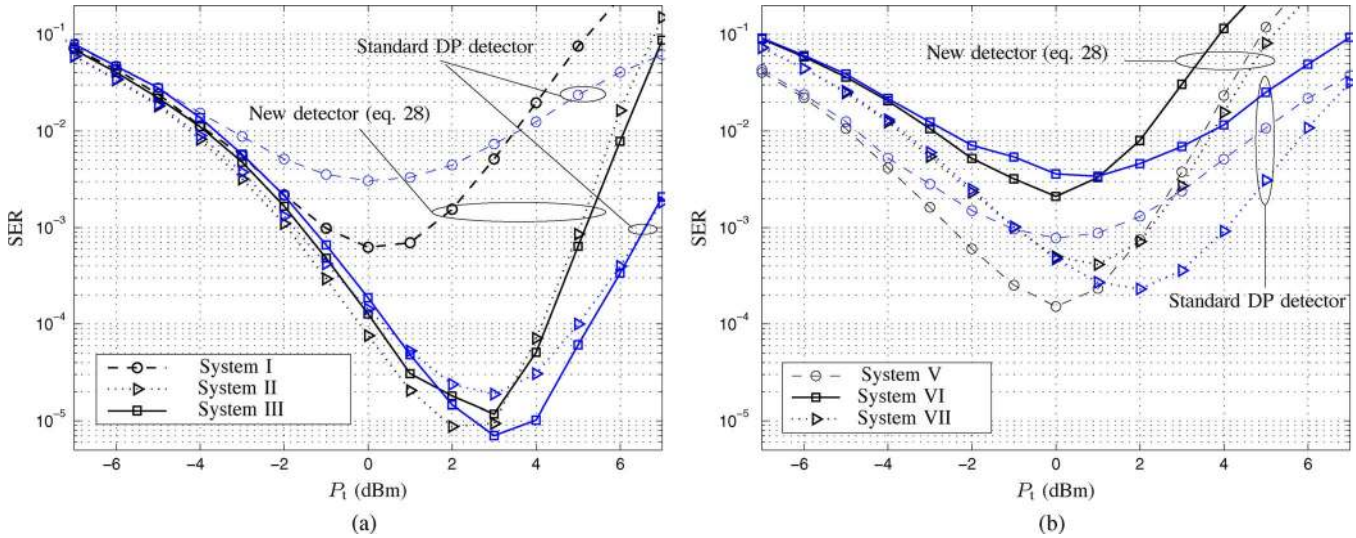

Fig. 4. SERs of systems (a) I–III, (b) V–VII with two different detectors versus transmitted power per polarization P_t.

systems with dispersion coefficients of 3 and 16.5 ps/nm/km for a range of symbol rates that the pdf changes from a shape close to our theoretical result to a Gaussian-like pdf. One may use a measure of similarity between the two pdfs, i.e., the numerical pdf of a DM link, extracted based on the NLSE and the theoretical pdf for a fiber-optic channel with low dispersion, derived in Theorem 1. Since the numerical calculation of the pdf tails is cumbersome, applying such measures of similarity like the Kullback–Leibler distance ([31] p. 251) are not feasible.

Instead, we only measure the advantage of using the theoretical pdf rather than the Gaussian pdf quantitatively by computing the SER using two different detectors: The detector based on (28) and a standard DP receiver with ideal polarization demultiplexing and phase synchronization. Since the decision boundaries in the standard receiver are assumed to be straight lines, its performance is optimal for Gaussian-like pdf. On the other hand, a new detector based on (28) outperforms the standard receiver for a non-Gaussian (bean-like) pdf. Moreover, we perform the SER comparison for two different types of fibers. In low-dispersion fibers, e.g., systems I–III as seen in Fig. 4(a), the new detector shows better results for 6 Gbaud, while at 15 Gbaud, the standard receiver outperforms the new detector. Therefore, the theoretical pdf is not accurate for symbol rates above 10 Gbaud. An analogous interpretation from Fig. 4(b) reveals that this threshold is even smaller for $D = 16.5$ ps/nm/km (systems V–VII). Moreover, we plotted the numerical marginal pdf of the received signal in one polarization, e.g., x, of the received signal for four different systems. Fig. 5(a)–(d) shows the pdf plots for (a) a system without dispersion (the same system as Fig. 3), (b) I, (c) system II, and (d) system IV, at $P_t = 1$ dB·m. The numerical pdf is close to the theoretical one for system without dispersion and I, but as seen in system II and, particularly, in system IV by increasing symbol rate, the pdf converges to a Gaussian-like pdf, as was previously reported in [11], [15]. Hence, this pdf can be approximated very well by a Gaussian pdf for symbol rates higher 7 and 20 Gbaud for systems with dispersion coefficients of 3 and 16.5 ps/nm/km, respectively. A Gaussian pulse shape filtering and its matched filter are considered for all simulations at the transmitter and the receiver, respectively. The corresponding number of spans in Table I were chosen such that the performance of the given systems can be evaluated with reasonable Monte Carlo complexity.

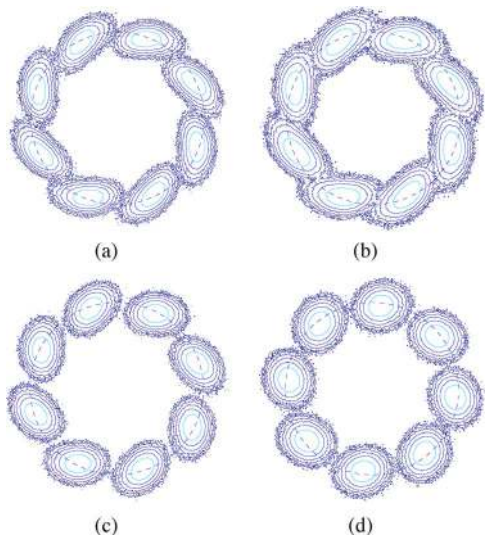

Fig. 5. Marginal joint pdf of the received phase and amplitude in one polarization, e.g., x at transmit power $P_t = 1$ dB·m for (a) system without dispersion (the same system as Fig. 3), (b) system I, (c) system II, and (d) system IV. The corresponding values of the contours are the same for all subfigures.

VI. Conclusion

The signal statistics of a DP fiber channel including the pdf of the NLPN and the joint probability of the received amplitudes and phases given the SNR of both polarizations have been derived. This makes it possible, for the first time, to analytically evaluate the performance of data transmission systems over DP fiber channels with phase noise and low enough symbol rate, and to optimize the performance of such systems. Moreover, a quantitive approach is proposed to measure the accuracy of the analytically derived pdf for a specific DM fiber-optical link.

APPENDIX
PROOF OF THEOREM 1

Before going into the detail of the proof of Theorem 1, we define the partial characteristic function by

$$\mathcal{F}^{-1}_{\omega_3\to r}\left\{\Psi_{\Theta_1,\Theta_2,R}(\omega_1,\omega_2,\omega_3)\right\} = \int_{-\infty}^{\infty}\Psi_{\Theta_1,\Theta_2,R}(\omega_1,\omega_2,\omega_3)e^{-jr\omega_3}d\omega_3$$

where $\mathcal{F}^{-1}_{\omega_3\to r}$ denotes the inverse Fourier transform with respect to ω_3 and the characteristic function $\Psi_{\Theta_1,\Theta_2,R}$ is given by

$$\Psi_{\Theta_1,\Theta_2,R}(\omega_1,\omega_2,\omega_3) = \int_0^{2\pi}\int_0^{2\pi}\int_0^{\infty} f_{\Theta_1,\Theta_2,R}(\theta_1,\theta_2,r) \times e^{j(\theta_1\omega_1+\theta_2\omega_2+r\omega_3)}d\theta_1 d\theta_2 dr. \quad (29)$$

Moreover, we introduce the following lemma, which will be used later.

Lemma 1: The 2-D Fourier series coefficient[5] $C_{\mathbf{k}}(r)$ of the joint pdf $f_{\Theta_1,\Theta_2,R}(\theta_1,\theta_2,r)$ with respect to θ_1 and θ_2 over $[0,2\pi)$ is obtained by

$$C_{\mathbf{k}}(r) = \frac{1}{4\pi^2}\mathcal{F}^{-1}_{\eta\to r}\left\{\Psi_{\Theta_1,\Theta_2,R}(-k_1,-k_2,-\eta)\right\}$$

where $\mathbf{k}=(k_1,k_2)$ is a vector with integer elements.

Proof: According to the definition of the partial characteristic function

$$\begin{aligned}&\mathcal{F}^{-1}_{\omega_3\to r}\left\{\Psi_{\Theta_1,\Theta_2,R}(\omega_1,\omega_2,\omega_3)\right\}\\ &\quad=\mathcal{F}_{(\theta_1,\theta_2)\to(\omega_1,\omega_2)}\left\{f_{\Theta_1,\Theta_2,R}(\theta_1,\theta_2,r)\right\}\\ &\quad=\int_0^{2\pi}\int_0^{2\pi} f_{\Theta_1,\Theta_2,R}(\theta_1,\theta_2,r)e^{-j(k_1\theta_1+k_2\theta_2)}d\theta_1 d\theta_2.\end{aligned} \quad (30)$$

Exploiting (30), the definition of the Fourier series coefficients

$$C_{\mathbf{k}}(r) = \frac{1}{4\pi^2}\int_0^{2\pi}\int_0^{2\pi} f_{\Theta_1,\Theta_2,R}(\theta_1,\theta_2,r) \times e^{-j(k_1\theta_1+k_2\theta_2)}d\theta_1 d\theta_2$$

and (29), the proof is complete. ■

Proof of Theorem 1: Since ϕ_x and $\hat{\mathbf{u}}_x$ are independent of ϕ_y and $\hat{\mathbf{u}}_y$, the joint characteristic function of the normalized NLPN ϕ_n and the linear part of the electric field $\hat{\mathbf{u}}$ with polar coordinates can be written as

$$\Psi_{\Phi_n,\hat{\mathbf{\Theta}},\mathbf{R}}(\nu,\mu,\eta) = \Psi_{\Phi_x,\hat{\Theta}_x,R_x}(\nu,\mu_x,\eta_x) \times\Psi_{\Phi_y,\hat{\Theta}_y,R_y}(\nu,\mu_y,\eta_y) \quad (31)$$

where $\mu=(\mu_x,\mu_y)$ and $\eta=(\eta_x,\eta_y)$. Hence, by taking the inverse Fourier transform, we get

$$\mathcal{F}^{-1}_{\eta\to\mathbf{r}}\left\{\Psi_{\Phi_n,\hat{\mathbf{\Theta}},\mathbf{R}}\right\} = \mathcal{F}^{-1}_{\eta_x\to r_x}\left\{\Psi_{\Phi_x,\hat{\Theta}_x,R_x}\right\}\mathcal{F}^{-1}_{\eta_y\to r_y}\left\{\Psi_{\Phi_y,\hat{\Theta}_y,R_y}\right\}. \quad (32)$$

On the other hand, using the results in ([20] p. 225), we have

$$\mathcal{F}^{-1}_{\eta_x\to r_x}\left\{\Psi_{\Phi_x,\hat{\Theta}_x,R_x}(\nu,\mu_x,\eta_x)\right\} = \frac{r_x\Psi_{\Phi_x}(\nu)}{\tau^2(\nu)} \times\exp\left(-\frac{r_x^2+m_x^2(\nu)}{2\tau^2(\nu)}\right)I_{\mu_x}\left(\frac{r_x m_x(\nu)}{\tau^2(\nu)}\right). \quad (33)$$

One may replace x with y in (33) to obtain $\mathcal{F}^{-1}_{\eta_y\to r_y}\{\Psi_{\Phi_y,\hat{\Theta}_y,R_y}\}$ and then, by substituting it and (33) into (32), we get

$$\mathcal{F}^{-1}_{\eta\to\mathbf{r}}\left\{\Psi_{\Phi_n,\hat{\mathbf{\Theta}},\mathbf{R}}(\nu,\mu,\eta)\right\} = \frac{r_x r_y\Psi_{\Phi_n}(\nu)}{\tau^4(\nu)} \times e^{-\frac{\|\mathbf{r}\|^2+\|\mathbf{m}(\nu)\|^2}{2\tau^2(\nu)}}I_{\mu_x}\left(\frac{r_x m_x(\nu)}{\tau^2(\nu)}\right)I_{\mu_y}\left(\frac{r_y m_y(\nu)}{\tau^2(\nu)}\right). \quad (34)$$

The partial characteristic function (see Definition 1) of the received phase vector θ and amplitude vector $\mathbf{r}$ of the received signal can be computed by

$$\mathcal{F}_{\theta\to\nu}\{f_{\mathbf{\Theta},\mathbf{R}}(\theta,\mathbf{r})\} = \mathcal{F}^{-1}_{\mu\to\mathbf{r}}\{\Psi_{\mathbf{\Theta},\mathbf{R}}(\nu,\mu)\}. \quad (35)$$

Now, one may use (35) to find the coefficients of the 2-D Fourier series expansion of

$$f_{\mathbf{\Theta},\mathbf{R}}(\theta,\mathbf{r}) = \frac{1}{4\pi^2}\sum_{k_x=-\infty}^{\infty}\sum_{k_y=-\infty}^{\infty}C_{\mathbf{k}}(\mathbf{r})e^{j\mathbf{k}\cdot\theta} \quad (36)$$

with respect to θ for a given r_x and r_y. Therefore, using (22), (35), and Lemma 1, these Fourier series coefficients $C_{\mathbf{k}}$ are obtained as

$$\begin{aligned}C_{\mathbf{k}}(\mathbf{r}) &= \mathcal{F}^{-1}_{\eta\to\mathbf{r}}\{\Psi_{\mathbf{\Theta},\mathbf{R}}\}(-\mathbf{k},\mathbf{r})\\ &= \mathcal{F}^{-1}_{\eta\to\mathbf{r}}\left\{\Psi_{\Phi_n,\hat{\mathbf{\Theta}},\mathbf{R}}\right\}(k_x+k_y,-\mathbf{k},\mathbf{r}).\end{aligned} \quad (37)$$

Substituting (34) into (37), one can get (24). On the other hand, exploiting $C_{-\mathbf{k}}=C_{\mathbf{k}}{}^{\dagger}$, where † denotes the complex conjugate, $C_{(0,0)}=f_{\mathbf{R}}(\mathbf{r})$, and some algebraic manipulations on (36), one can obtain (23). ■

[5]Although the joint pdf $f_{\mathbf{\Theta},\mathbf{R}}$ is not a periodic function of θ, in order to use the Fourier series expansion, we assume this pdf function is equivalent to a periodic function only in its one period where θ_x and θ_y are confined to the range of $[0,2\pi)$.

ACKNOWLEDGMENT

The authors gratefully acknowledge the anonymous reviewers for the insightful comments and constructive suggestions.

REFERENCES

[1] K. Roberts, M. O'Sullivan, K.-T. Wu, H. Sun, A. Awadalla, D. J. Krause, and C. Laperle, "Performance of dual-polarization QPSK for optical transport systems," *J. Lightw. Technol.*, vol. 27, no. 16, pp. 3546–3559, Aug. 2009.

[2] T. Pfau, S. Hoffmann, O. Adamczyk, R. Peveling, V. Herath, M. Porrmann, and R. Noé, "Coherent optical communication: Towards real-time systems at 40 Gbit/s and beyond," *Opt. Exp.*, vol. 16, no. 2, pp. 866–872, Jan. 2008.
[3] P. Winzer, "Beyond 100G ethernet," *IEEE Commun. Mag.*, vol. 48, no. 7, pp. 26–30, Jul. 2010.
[4] L. E. Nelson, S. L. Woodward, S. Foo, M. Moyer, D. J. S. Beckett, M. O'Sullivan, and P. D. Magill, "Detection of a single 40 Gb/s polarization-multiplexed QPSK channel with a real-time intradyne receiver in the presence of multiple coincident WDM channels," *J. Lightw. Technol.*, vol. 28, no. 20, pp. 2933–2943, Oct. 2010.
[5] R. J. Essiambre, G. Kramer, P. J. Winzer, G. J. Foschini, and B. Goebel, "Capacity limits of optical fiber networks," *J. Lightw. Technol.*, vol. 28, no. 4, pp. 662–701, Feb. 2010.
[6] A. D. Ellis, J. Zhao, and D. Cotter, "Approaching the non-linear Shannon limit," *J. Lightw. Technol.*, vol. 28, no. 4, pp. 423–433, Feb. 2010.
[7] H. Bülow, "Polarization QAM modulation (POL-QAM) for coherent detection schemes," in *Proc. Opt. Fiber Commun. Conf.*, Mar. 2009, pp. 1–3, OWG2.
[8] E. Agrell and M. Karlsson, "Power-efficient modulation formats in coherent transmission systems," *J. Lightw. Technol.*, vol. 27, no. 22, pp. 5115–5126, Nov. 2009.
[9] G. P. Agrawal, *Nonlinear Fiber Optics*, 4th ed. New York: Academic, 2007.
[10] J. P. Gordon and L. F. Mollenauer, "Phase noise in photonic communications systems using linear amplifiers," *Opt. Lett.*, vol. 15, no. 23, pp. 1351–1353, 1990.
[11] A. Bononi, P. Serena, and N. Rossi, "Modeling of signal-noise interactions in nonlinear fiber transmission with different modulation formats," *Opt. Fiber Technol.*, vol. 16, no. 2, pp. 73–85, 2010.
[12] A. Mecozzi, "Limits to long-haul coherent transmission set by the Kerr nonlinearity and noise of the in-line amplifiers," *J. Lightw. Technol.*, vol. 12, no. 11, pp. 1993–2000, Nov. 1994.
[13] K.-P. Ho, "Probability density of nonlinear phase noise," *J. Opt. Soc. Am. B*, vol. 20, no. 9, pp. 1875–1879, 2003.
[14] Y. Yadin, M. Shtaif, and M. Orenstein, "Nonlinear phase noise in phasemodulated WDM fiber-optic communications," *IEEE Photon. Technol. Lett.*, vol. 16, no. 5, pp. 1307–1309, May 2004.
[15] P. Serena, A. Orlandini, and A. Bononi, "Parametric-gain approach to the analysis of single-channel DPSK/DQPSK systems with nonlinear phase noise," *J. Lightw. Technol.*, vol. 24, no. 5, pp. 2026–2037, May 2006.
[16] H. Kim and A. H. Gnauck, "Experimental investigation of the performance limitation of DPSK systems due to nonlinear phase noise," *IEEE Photon. Technol. Lett.*, vol. 15, no. 2, pp. 320–322, Feb. 2003.
[17] A. Mecozzi, "Probability density functions of the nonlinear phase noise," *Opt. Lett.*, vol. 29, no. 7, pp. 673–675, 2004.
[18] S. Kumar, "Analysis of nonlinear phase noise in coherent fiber-optic systems based on phase shift keying," *J. Lightw. Technol.*, vol. 27, no. 21, pp. 4722–4733, Nov. 2009.
[19] A. Demir, "Nonlinear phase noise in optical-fiber-communication systems," *J. Lightw. Technol.*, vol. 25, no. 8, pp. 2002–2032, Aug. 2007.
[20] K.-P. Ho, *Phase-Modulated Optical Communication Systems*. New York: Springer-Verlag, 2005.
[21] A. P. T. Lau and J. M. Kahn, "Signal design and detection in presence of nonlinear phase noise," *J. Lightw. Technol.*, vol. 25, no. 10, pp. 3008–3016, Oct. 2007.
[22] K.-P. Ho and J. Kahn, "Electronic compensation technique to mitigate nonlinear phase noise," *J. Lightw. Technol.*, vol. 22, no. 3, pp. 779–783, Mar. 2004.
[23] D. Wang and C. Menyuk, "Polarization evolution due to the Kerr nonlinearity and chromatic dispersion," *J. Lightw. Technol.*, vol. 17, no. 12, pp. 2520–2529, Dec. 1999.
[24] G. Charlet, N. Maaref, J. Renaudier, H. Mardoyan, P. Tran, and S. Bigo, "Transmission of 40 Gb/s QPSK with coherent detection over ultra-long distance improved by nonlinearity mitigation," in *Proc. Eur. Conf. Exhib. Opt. Commun.*, 2006, Paper Th4.3.4.
[25] C. Xu and X. Liu, "Postnonlinearity compensation with data-driven phase modulators in phase-shift keying transmission," *Opt. Lett.*, vol. 27, no. 18, pp. 1619–1621, 2002.
[26] G. Grimmett and D. Stirzaker, *Probability and Random Processes*, 3rd ed. London, U.K.: Oxford Univ. Press, 2001.
[27] A. Bononi, P. Serena, and N. Rossi, "Nonlinear limits in single- and dual-polarization transmission," in *Proc. LEOS Summer, Topicals*, 2010, pp. 38–39, Paper TuA3.3.
[28] J. G. Proakis and M. Salehi, *Digital Communications*, 5th ed. New York: McGraw-Hill, 2008.
[29] M. Karlsson and E. Agrell, "Which is the most power-efficient modulation format in optical links?," *Opt. Exp.*, vol. 17, no. 13, pp. 10814–10819, Jun. 2009.
[30] G. Charlet, J. Renaudier, O. B. Pardo, P. Tran, H. Mardoyan, and S. Bigo, "Performance comparison of singly-polarized and polarization multiplexed at 10Gbaud under nonlinear impairments," presented at the presented at the Opt. Fiber Commun. Conf./Natl. Fiber Opt. Eng. Conf., San Diego, CA, 2008, Paper OThU8.
[31] T. M. Cover and J. A. Thomas, *Elements of Information Theory*, 2nd ed. New York: Wiley-Interscience, 2006.

Lotfollah Beygi received the B.Sc. and M.Sc. degrees in electrical engineering from the University of Tehran, Tehran, Iran, in 1999 and 2002, respectively. Since 2008, he has been working toward the Ph.D. degree in the Communication Systems and Information Theory Group, Chalmers University of Technology, Gothenburg, Sweden.

From 2003 to 2008, he was with the R&D division of Jooyandegan Fannavari Ettelaat. His main research interests include coded modulation and digital signal processing for fiber-optical and wireless communications.

Erik Agrell received the M.Sc. degree in electrical engineering and the Ph.D. degree in information theory from the Chalmers University of Technology, Gothenburg, Sweden, in 1989 and 1997, respectively.

From 1988 to 1990, he was with Volvo Technical Development as a Systems Analyst, and from 1990 to 1997, with the Department of Information Theory, Chalmers University of Technology, as a Research Assistant. In 1997–1999, he was a Postdoctoral Researcher with the University of Illinois at Urbana-Champaign and the University of California, San Diego. In 1999, he joined the Faculty of the Chalmers University of Technology as an Associate Professor, where he has been a Professor in communication systems since 2009. His current research interests include coding, modulation, and equalization for fiber-optic channels, bit-interleaved coded modulation, and multilevel coding, bit-to-symbol mappings in coded and uncoded systems, lattice theory and sphere decoding, and multidimensional geometry.

Dr. Agrell served as the Publications Editor for IEEE TRANSACTIONS ON INFORMATION THEORY from 1999 to 2002.

Magnus Karlsson received the Ph.D. degree in electromagnetic field theory from the Chalmers University of Technology, Gothenburg, Sweden, in 1994. The title of his Ph.D. thesis was "Nonlinear propagation of optical pulses and beams."

Since 1995, he has been with the Photonics Laboratory, Chalmers University of Technology, first as an Assistant Professor and since 2003 as a Professor in photonics. He is the author or coauthor of more than 190 scientific journal and conference contributions. His research has been devoted to a variety of aspects of fiber-optic communication systems, in particular, transmission effects such as fiber nonlinearities and polarization effects, but also applied issues such as high-capacity data transmission and all-optical switching. Currently he is devoted to parametric amplification, multilevel modulation formats, and coherent transmission in optical fibers.

Dr. Karlsson served as the Guest Editor for the JOURNAL OF LIGHTWAVE TECHNOLOGY, and is currently the Associate Editor of *Optics Express*. He has served in the technical committees for the Optical Fiber Communication Conference (2009 as the Subcommittee Chair), and the Asia Communications and Photonics Conference.

Pontus Johannisson received the Ph.D. degree from the Chalmers University of Technology, Gothenburg, Sweden, in 2006. His thesis was focused on nonlinear intrachannel signal impairments in optical fiber communications systems.

In 2006, he joined the Research Institute IMEGO in Gothenburg, Sweden, where he was involved in digital signal processing for inertial navigation with microelectromechanical systems based accelerometers and gyroscopes. In 2009, he joined the Photonics Laboratory, Chalmers University of Technology, where he is currently an Assistant Professor. His research interests include nonlinear effects in optical fibers and digital signal processing in coherent optical receivers.